CANDU-Specific Severe Core Damage Accident Experiments in Support of Level 2 PSA

P.M. Mathew [1)], W.C.H. Kupferschmidt[2)], V.G. Snell[3)] and M. Bonechi[4)]
1) Atomic Energy of Canada Ltd., Whiteshell Laboratories, Pinawa, Manitoba, Canada, R0E 1L0
2) Atomic Energy of Canada Ltd., Chalk River Laboratories, Chalk River, Ontario Canada, K0J 1J0
3,4) Atomic Energy of Canada Ltd., Sheridan Park Research Community, 2251 Speakman Drive, Mississauga, Ontario, Canada, L5K 1B2

ABSTRACT

This paper describes progress made in CANDU severe core damage accident experiments conducted with a single channel of one-fifth scale containing twelve simulated fuel bundles in an inert atmosphere. The geometry of the reference fuel channel considered in this study is a pressure tube-calandria tube composite, with the pressure tube ballooned into circumferential contact with the calandria tube. The tests are conducted to develop a better understanding of the behaviour of a CANDU fuel channel array when the CANDU reactor core undergoes a postulated, low probability severe core damage accident. The data are required to ensure that the core damage models used in MAAP CANDU code are adequate. MAAP CANDU code is used to calculate the progression of a severe core damage accident in a CANDU reactor to support Level 2 Probabilistic Safety Assessment (PSA) activities.

Experimental results from this study showed the development of time-dependent sag when the reference channel temperature exceeds 800^0C, thus suggesting that creep is the mode of channel deformation. Significant localized wall thinning and high longitudinal strain localization were observed at the bundle junctions along the bottom-side of the channel, at a distance one to two bundles away from the channel mid-point. Thus the debris formed by this mechanism is expected to be two to three bundles long. A creep-assisted deformation mechanism is proposed to support the findings. The experiments showed that the end-load applied by the channel during heat-up and during cool-down is small. Scaling up the data showed that the forces are not sufficient to pull a full-size CANDU channel out from the end-fitting. Therefore, it may be possible to pump coolant into the channel for accident management, without inducing failure of the channel during the early stages of the sag phenomena prior to the development of significant wall-thinning at the bundle junctions.

INTRODUCTION

The CANDU reactor utilizes the fuel channel concept, which consists of an array of horizontal fuel channels, containing fuel bundles and heavy water coolant, passing through a large horizontal, cylindrical calandria vessel filled with heavy water moderator. Figure 1 shows a schematic of the arrangement of fuel bundles and fuel channels inside calandria. The calandria is surrounded by a shield tank with a large volume of light water, which is not shown in the figure.

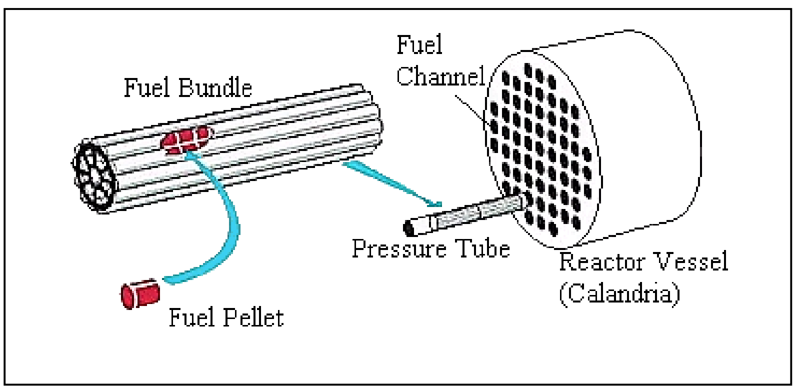

Fig. 1 Schematic of a CANDU Reactor Core Showing the Fuel Channel Concept

In postulated severe accident sequences in a CANDU reactor—as for example, a loss of coolant, plus unavailability of the emergency core-cooling system—the separately cooled moderator provides an effective heat sink. The moderator has an active heat removal capacity of about 5% thermal power, which is sufficient to remove decay heat shortly after shutdown. The moderator cooling, therefore, can prevent gross melting of the fuel and maintain fuel channel integrity. In addition to the adequate heat removal capability of the moderator, the local subcooling should be sufficient to prevent overheating and failure of the calandria tube on pressure-tube contact. Prevention of prolonged film boiling on the calandria tube surface is adequate to prevent channel failure [1].

There is, however, a very low probability that the moderator system itself could also be unavailable. Under such a low probability accident scenario, for example, in a Station Blackout scenario with loss of all AC power, including both sets (Group 1 and Group 2) of redundant emergency diesel generators, the fuel channels are uncovered during moderator boil-off and will gradually sag and break-up forming debris. Even in such accidents, called "Severe Core Damage Accidents", the debris will be contained within the calandria as long as it remains cooled on the outside by the shield-tank water [2,3,4]. The slow boil-off of the shield tank water will delay the failure of the calandria vessel for about a day. This delay allows the operator sufficient time to implement severe accident management measures. The CANDU core disassembly experiments, described in this paper, address the behaviour of CANDU channels during moderator boil-off, when the channels are expected to sag under heat-up and to break up to form debris [5]. A sagging channel eventually contacts the lower channel and if the lower channel is also uncovered it is expected to sag under its own weight as well as that of the supported channel. This process would continue, as more channels are uncovered. As sagging increases, it is expected that the channel segments separate near the bundle junctions. A suspended debris bed is thus formed, which moves downward with the falling moderator level. The submerged channels will be able to support a finite number of channels after which they are also expected to fail. The loading on the submerged channels increases with the accumulation of debris from top channels, thereby leading to progressive failure of the lower channels and ultimately resulting in the collapse of the core into the moderator pool in the bottom of the calandria.

In a first step to understand the core disassembly phenomenon, single channel disassembly tests were conducted in an inert atmosphere to study channel deformation, failure and disassembly mechanisms. The results of those tests are reported here. Because of the prohibitive costs to conduct full-scale tests, the full-size channel was suitably scaled down to a manageable size by using a scaling analysis based on geometric and stress-level similarity.

In terms of analysis of these sequences, AECL and Ontario Power Generation Inc. are developing the MAAP-CANDU code to conduct severe core damage accident consequence analysis for CANDU reactors [6]. MAAP CANDU is the CANDU-version of the MAAP PWR code. AECL is applying this code to CANDU 6 and CANDU 9 plants. This code uses a number of system and component failure criteria to analyze the progression and consequences of a postulated severe core damage accident. Many of the failure criteria currently used in the code, which are generic to both PWR and CANDU, are supported by experiments. But severe accident experiments, specific to the CANDU geometry are lacking. Therefore, AECL is conducting CANDU-specific experiments to address this gap in knowledge. This paper describes progress made in CANDU core disassembly experiments, which are conducted to develop a better understanding of the behaviour of a CANDU fuel channel array when it undergoes a severe core damage accident.

SCALING METHODOLOGY

The geometry of the fuel channel considered in this study is a pressure tube-calandria tube composite, with the pressure tube ballooned into circumferential contact with the calandria tube. Factors that affect the channel deformation and failure are its stiffness, stress, creep behaviour, temperature distribution, restraint at ends and by lower channels, and physical and chemical processes, such as localized wall thinning, oxidation and melting of channel material. For the small-scale channel the pressure tube material Zirconium-2.5 wt% Niobium (Zr-2.5Nb) was chosen, because the pressure tube is thicker than the calandria tube, which is made of Zircaloy-2. The creep and tensile properties of the CANDU pressure tube material was achieved in the small-scale channel by appropriate heat treatment processes. The stress, temperature distributions and end-restraints were replicated in the experiments. The remaining factors, stiffness and support by lower channels, are addressed through scaling. Interference between the ballooned pressure tube-calandria tube and the fuel bundles is not expected during the early stages of channel deformation because of the large radial clearance between the bundle and the pressure tube. Therefore, tube stiffness is a function of the tube dimensions only. As mentioned above, the tests reported here were conducted in an inert atmosphere to understand the deformation and failure mechanisms of a single channel; the effect of oxidation will be addressed in separate tests.

In the calculations, a scaling methodology to maintain geometric similarity between the full size and the small-scale channel was applied. In this method, a constant scaling ratio of the significant dimensions of the full-size channel is maintained in the scaled-down geometry. Since the main goal of the tests was to study the deformation and failure

mechanisms of the channel, the stress level of the full-size channel was maintained in the small-scale channel, so that those mechanisms are scale-independent. Scaling calculations showed that the simulated fuel bundles (heaters) inside the small-scale experimental channel required a high-density material to maintain the high stress levels of the full-size channel. Also, the simulated bundle material had to withstand high temperatures. Therefore, the heaters were made of tungsten. Table 1 summarizes the parameters of a full-size CANDU 6 channel, the small-scale channel and the scaling ratio. It shows that,

Table 1. Dimensions of a CANDU 6 Channel, Small-Scale Experimental Channel and the Scaling and Aspect Ratios

Parameter	CANDU 6 Channel	Small-scale Test Channel	Scaling Ratio
Channel Length (m)	5.994	1.2	5.0
Channel Vert. Separation (mm)	160	32	5.0
Channel ID (mm)	122.1	24.1	5.1
Bundle O.D. (mm)	102.8	20.8	4.9
Bundle Length (mm)	495.3	99	5.0
Bundle-Channel Gap (mm)	19.3	3.3	5.8
Wall Thickness (mm)	5.0	0.4	12.5
Max. Stress at Mid-span (MPa)	14.5	14.5	1.0
Channel Aspect ratio (L/D)	49	50	1.0
Bundle Aspect Ratio (L/D)	4.9	4.8	1.0

except for the wall thickness, an approximate scaling ratio of 1:5 could be maintained. The wall thickness scaling is not an important issue in the current tests, because these tests are conducted in inert to understand the channel deformation mechanism. However, in future tests when an oxidizing atmosphere is used, the oxidation behaviour of the channel will be simulated by an appropriately scaled heat-up rate. Based on the scaling calculations, an experimental facility was designed and built. Also pre-test calculations were conducted with a simple model to determine the influence of various parameters on channel sag.

PRE-TEST CALCULATIONS

As a first step to model the experiment, a simple numerical model was developed using ABAQUS, which is a finite element code for numerical analysis of mechanical and/or thermal problems. The model was used to conduct sensitivity studies to determine the effect of various experimental parameters on channel sag. The experimental channel was modelled as a beam, with one end of the beam fixed in the axial direction and against rotation around the vertical plane. The other end was allowed to move freely outward in the axial direction during heat up, but was restrained to move back beyond the original location. These are boundary conditions of the actual CANDU channel, which were maintained as such in the test channel. Two approaches were used to model the sag behaviour. In the first simple model, the inelastic deformations were modelled as time-dependent caused by yielding of the material (Plasticity Model); and in the second model, time-dependent creep deformation was implemented. One test case was run with each model for a slow heat-up rate of ~0.2^{0}C/s from 300 to 1400^{0}C. The results showed that the maximum sag was ~12% higher for the creep model; but both models predicted a similar pattern for the general sag behaviour. Because the plasticity model took only a very short time to run (~5 min.) compared to 3 hours for the creep model, the plasticity model was used for the sensitivity studies.

The influence of axial temperature profile (heated length) was calculated assuming that only 4, 8, or 10 of the 12 heaters were powered. For a short heated length (4 and 8 heaters), the maximum sag is approximately proportional to the heated length raised to the fourth power and for a longer heated length (8 and 10 heaters) the maximum sag is almost linearly proportional to the heated length. Therefore, knowledge of the heated length is critical in predicting the sag behaviour. The effect of circumferential temperature gradient across the diameter of the circular section of the channel with 10 powered heaters was examined in two sensitivity studies. In one case, the temperature of the top of the channel was assumed 200^{0}C lower than the bottom. In the second case, the channel was assumed isothermal. The sag increase for the isothermal channel was small, ~8% only. This difference is attributed to the decrease in material strength with increasing temperature. The modelling results showed that the inclusion of axial restraint at the floating end in the model, when the channel returns to the original position, is very important to preserve the integrity of the channel at high temperature. With increasing sag, the channel is restrained at the original position, resulting in a significant increase in the horizontal reaction force. This second order effect of the axial reaction, which is equal to the horizontal force multiplied by the sag, restricts the sag at high temperature.

EXPERIMENTAL DETAILS

Description of the Core Disassembly Test Facility

Based on the scaling calculations and the design requirements, a one-fifth linear-scale Core Disassembly Test Facility (CDF) was built and commissioned at the AECL Whiteshell Laboratories. The facility allows testing of up to four channels of a vertical section of the core, as shown in the flow diagram of the facility in Figure 2 (see CDF Chamber). The CDF chamber is the heart of the facility, where the tests are conducted in a controlled atmosphere, after evacuating the chamber initially and backfilling it with the desired gas. Each scaled-down channel, about 1200 mm long and 25 mm in diameter, contains twelve one-fifth-scale heaters representing the twelve fuel bundles of the full-size channel, which is electrically insulated from the end supports. As in a full size channel, one end of the channel is fixed and the other end allows horizontal movement (floating end). The channels can be videotaped during a test through the water-cooled windows installed inside the chamber.

The power supply and control system of the facility consists of a 600V main power supply, with circuit splitters, transformers and switches (s. Figure 2). Each heater is fed with 60V, 30A, and there are two heaters per circuit. A maximum of ten centre heaters of the channel are powered and a maximum sheath temperature of 1400^{0}C can be achieved in a test. Various test data such as temperature (spot-welded thermocouples to sheath), channel end-load (load cell), sag at channel's mid-point (Laser device), channel longitudinal displacement (LVDT) and channel power (volt and current meters) are monitored using LABVIEW software.

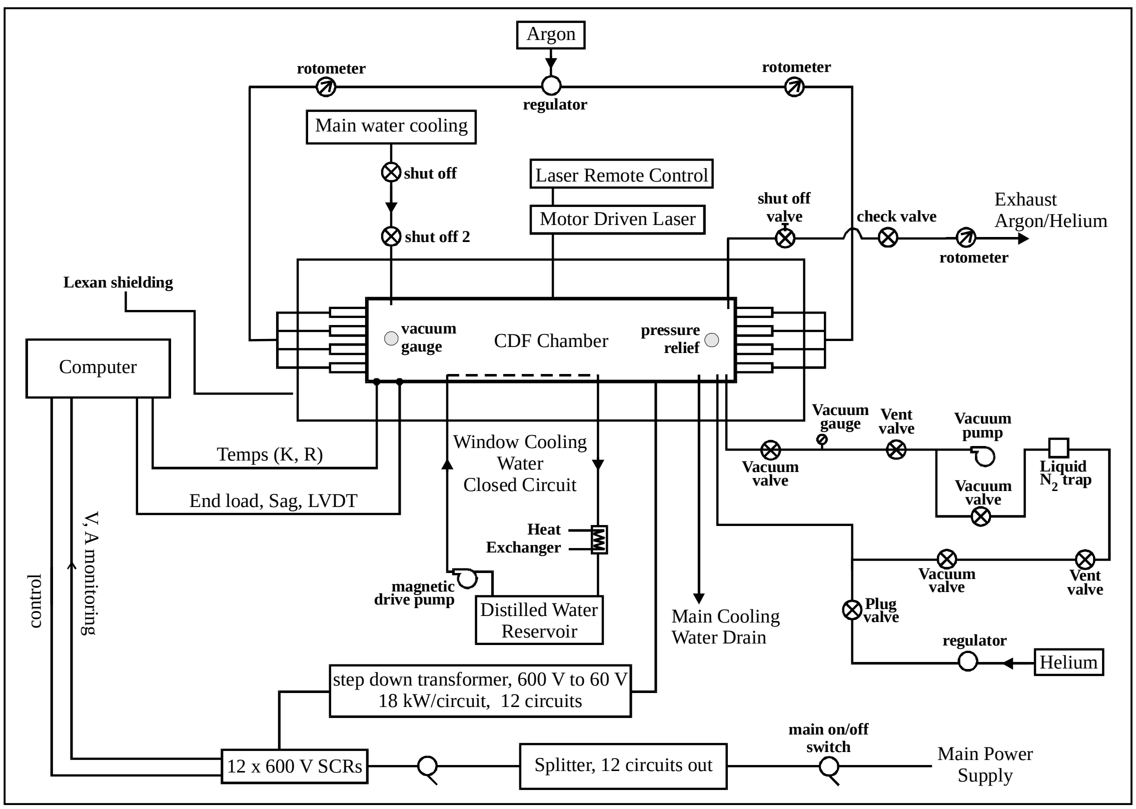

Fig. 2 A Flow Diagram of the CANDU Core Disassembly Test Facility

Test Procedure and Post-test Examination

In a typical test, the temperature of the channel is at first increased to the range of reactor operating temperature (~300^{0}C) and then held there until thermal equilibrium is reached. The power is then increased so that the channel reaches a maximum temperature in the range 1300 to 1400^{0}C. The heat-up rate up to the maximum temperature was varied in the different tests, in the range 0.1 to 1.2^{0}C/s. This range covers the heat-up rate of fuel channels when uncovered by the moderator. The channel was held at the maximum temperature for holding times in the range 600 to 5500 s. Tests were

conducted with power supplied to either four or ten of the central heaters. In addition to monitoring the various test data and videotaping, post-test examination of the channel was conducted in which the axial sag profile, any change to original diameter and wall-thickness along the top and bottom at various locations were measured. The channel was also radiographed to determine the post-test location of the heaters. Also, the localized axial strain at the bundle junctions along the bottom side was determined from the radiographs and the final bundle imprints at the bundle junctions.

RESULTS AND DISCUSSION

Five tests were conducted with a single channel in an argon atmosphere, where the channel was allowed to sag freely. A summary of the test results is shown in Table 2. Because, no significant sag was observed below 800°C, it was chosen as the base reference temperature, and the heat-up rate was calculated from the total time the channel spent above 800°C until the test was terminated by turning off the power (Table 2).

Table 2. Summary of Single Channel Test Results in Argon Atmosphere

Test No.	Number of Powered Heaters Per channel	Max. Temp. at Mid-point (°C)	Transient Max. Sag at mid-point (mm)	Permanent Max. Sag at mid-point (mm)	Heat-up Rate from 800°C (°C /s)
CD-3	4	1415	24	18	0.26
CD-4	10	1320	117	108	0.10
CD-5	10	1415	100	-	-
CD-6	10	1310	88	79	1.20
CD-7	10	1307	120	111	0.09

Figure 3 shows the measured sag for the tests CD-3 and CD-5. For those tests the maximum temperature was the same, 1415°C, but the number of powered heaters were 4 and 10 respectively. Figure 3 shows the significant effect of heated length on sag. When 10 heaters are powered, and the channel is heated to 1415°C, the channel sag at mid-point is large, ~100 mm. Since the vertical separation between the channels is 32 mm (see Table 1), the top channel will have sagged to touch the next channel underneath and transferred the load onto the second channel underneath. The tests also show, as mentioned above, that below 800°C the measured sag is very small.

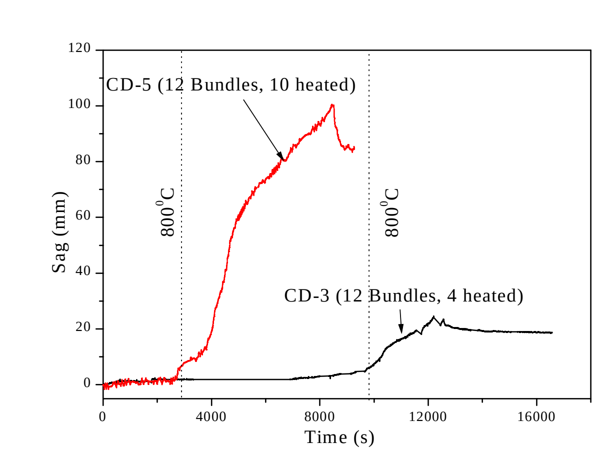

Fig. 3 Relationship Between Measured Sag at Channel Mid-point and Heated length

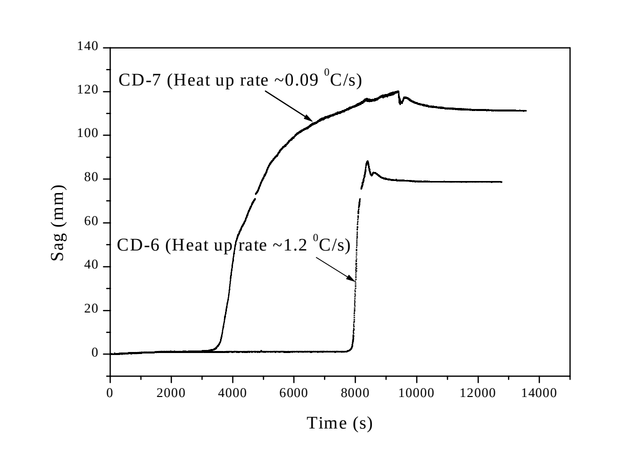

Fig. 4 Measured Sag for Two Tests with Different Heat up Rates

A comparison of the test results for CD-4 and CD-7 (see Table 2, same heated length of 10 powered heaters) shows that for the same heat up rate of ~0.1°C/s, and for the same maximum temperature range (1307-1320°C), the measured sag at channel mid-point is about the same (117-120 mm). These two tests show the good reproducibility of the test results.

The measured sag for CD-6 and CD-7 is shown in Figure 4. The maximum temperature and the heated length was the same (1307-1310 °C and 10 powered bundles) in both tests. Therefore, the results in Figure 4 show the effect of heat up rate on sag. A slow heat up gives higher sag, thus indicating that the time-dependent material creep to be the most important deformation mechanism during sag. An indication of the effect of creep on sag was noted in the pre-test calculations as mentioned earlier. Any future model development to explain the findings must, therefore, include the creep mechanism [7]. At present, such a model is under development. Table 2 shows that the permanent sag measured after the channel cooled down to room temperature, is in the range 6-9 mm less than the maximum transient sag measured at temperature. This decrease results from the thermal contraction during cooling.

An example of the details of the transient data obtained in a test, such as the top and bottom temperature 10 mm from channel mid-point, the load applied by the channel at the floating end, horizontal displacement and sag at mid-point are plotted in Figures 5 and 6 for test CD-7. A comparison of the Figures 5 and 6 shows, that sag increases significantly, only when the channel bottom temperature reaches ~800°C. The horizontal displacement curve in Figure 6 shows, as expected, a positive displacement of the floating end due to thermal expansion and a reversal at point "A," when the channel sag rate and displacement rate are equal. The end-load applied by the channel during sagging is small, less than 10 N. This force corresponds to less than 0.65 kN for the full-size channel, which is insufficient to pull the calandria tube out from the end-fitting. Therefore, no channel pull-out is expected as a result of the sag phenomenon. The force increases to about ~250 N during cooling, as shown in Figure 6. This force corresponds to ~16 kN for the full-size channel, which is again small for channel pull-out from the end-fitting. This suggests that in severe accident management it is still an option (if a source of water is available) to pump coolant into the channel during the early stage of the sag phenomena, before significant wall-thinning develops at the bundle junctions.

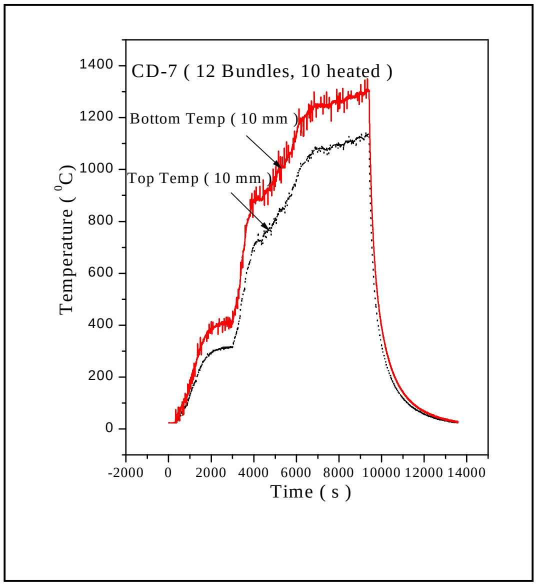

Fig. 5 Top and Bottom Temperature 10 mm from Channel Mid-point for Test CD-7

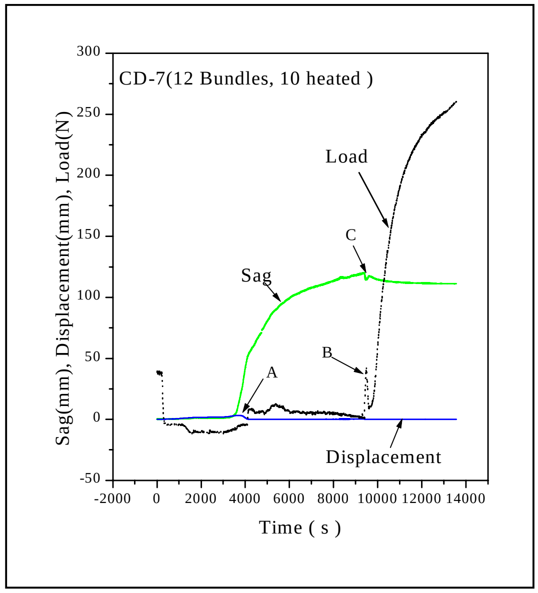

Fig. 6 Sag at Mid-point, Horizontal Displacement and End-load for Test CD-7

The peak at "B" in the load-curve and the coinciding valley observed at "C" in the sag-curve in Figure 6, observed during cool-down, is the result of alpha-to-beta phase transformation of Zr-2.5Nb. During this temperature range, the thermal expansion coefficient goes through a maximum and a minimum, which is reflected in the sag and load curves. The forces developed during this phase transformation are also insufficient to cause break up of the channel, if no significant prior wall-thinning occurred.

The channel was sectioned along the vertical axis and the wall thickness was measured along the top and bottom sides of the channel at different locations. Figure 7 shows the wall thickness plotted on a vertical projection of the sagged channel, measured from the fixed end. This figure shows that the bundles did not move from their original location relative

to the channel. Figure 7 also shows that in the centre region between two adjacent bundles, significant wall-thinning occurred at the bundle junctions along the bottom side of the channel. The thinnest wall thickness is not observed at the channel's mid-point (~600 mm in Figure 7), but at one to two bundles away from the channel's mid-point. This observation suggests, that the pressure-tube and calandria tube debris formed by this mechanism will be 2 to 3 bundles long. Furthermore, Figure 7 shows wall-thinning and strain localization at the channel top only at the first bundle junction from both ends. Because of the lower temperature of the channel end region, this thinning must have occurred under significantly higher stresses. This observation suggests that a CANDU channel may also fail at those locations along the top, if sufficiently high temperatures are reached. Figure 8 shows the average localized axial strain of the channel bottom at the bundle junctions as a function of the nominal distance from one end of the channel for the tests CD-6 and CD-7. In both tests, 10 of the 12 bundles were heated and the maximum temperature reached was in the range 1307 to 1310 °C. The strain measurements were made from the visible final imprint of the bundle location inside the channel, which were confirmed also from the post-test radiographs of the channel. The average strain plotted in Figure 8 was calculated from the imprint measurements and the original gap width between the bundles. The results in Figure 8 show that for CD-7 with the slower heat up rate the average localized strain at the bundle junctions is higher than for CD-6 with the higher heat up rate. Therefore, the deformation mechanism leading to wall thinning in the gap region is time-dependent creep. The results also show that, near the channel ends, the localized strain is higher for CD-7 than for CD-6. This is the result of the slow heat up rate in CD-7, where the channel ends reach higher temperatures due to axial heat conduction and thus produce a higher creep rate and higher strain in the end region. A comparison of the localized strain in Figure 8 for the two tests also show that the highest strain is not observed at the channel mid-point, but at a distance a bundle away from there. This observation is also consistent with the wall thickness measurements, shown in Figure 7. Figure 8 also shows that the localized strain at the channel bottom, one bundle away from the channel ends is very small. Failure at those locations along the channel topside is more likely, since wall thinning is greater at those locations along the topside of the channel as shown in Figure 6. As a result, channel stumps of a bundle long could remain attached to the end-fitting.

Measurements of the channel's outer diameters from front-to-back showed that the channel becomes oval in cross-section and near the bundle junctions the lower half of the channel conforms to the shape of the bundle, suggesting firm gripping of the bundles by the channel at those junctions during sag. As expected, away from the channel mid-point, where the temperature was lower, significantly less deviation from the original channel diameter is observed.

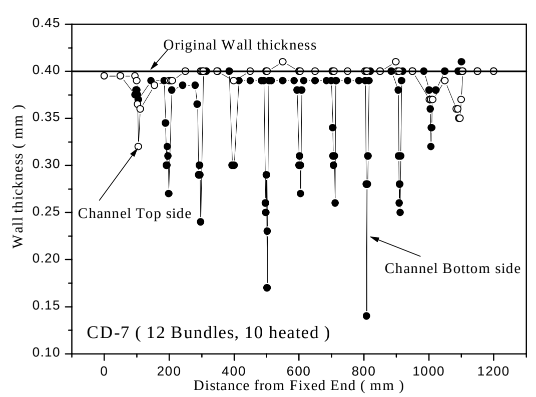

Fig. 7 Wall Thickness of the Top and Bottom Side of the Channel from Fixed End for Test CD-7

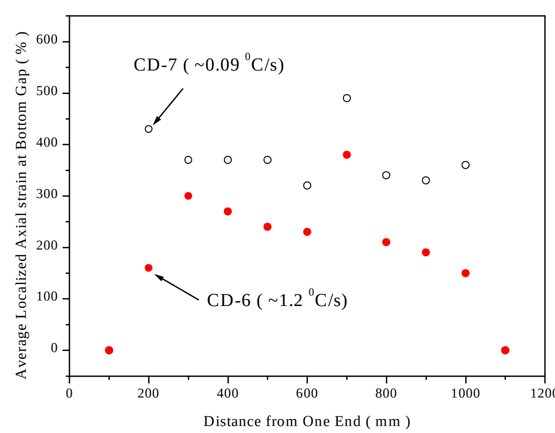

Fig. 8 Axial Localized Strain at Channel Bottom Bundle Junction Region for Tests CD-6 and CD-7

CONCLUSIONS

The behaviour of a CANDU channel under severe core damage accident sequences was investigated in a series of small-scale tests. Preliminary indications of the single-channel tests conducted in an inert atmosphere support previous hypotheses that the dominant mechanism is relatively slow creep-sag, leading to coarse debris as the channels slowly collapse. Specific findings to date are:

- The sag at channel's mid-point increases with heated length and significant sag occurs only above 800^{0}C.

- Sag is time-dependent, thus suggesting creep mechanism for channel deformation.
- Significant localized wall thinning was observed at the bundle junctions along channel bottom side at a distance, one to two bundles away from the channel mid-point. The pressure-tube and calandria tube debris formed by the disassembly of a CANDU core is thus expected to be two to three bundles long.
- Bundles do not move relative to the channel during sag. As channel temperature increases, the channel's lower-half grips the bundle tightly at both ends of the bundle at the bundle junctions. Sagging of the channel continues and the bundle moves with the channel. The sagged channel takes the shape of a cord, held at both ends. The channel material between the bundles locally deforms, which is associated with significant wall-thinning of the bundle-to-bundle gap region and high localized strain concentration, weakening of the region, leading to break up and debris formation.
- The end-load applied by the channel during sagging and during cooling is small, not sufficient to pull out the channel from the end-fitting. Therefore, if an alternate supply of water is available, it may be better to pump coolant into the channel during early stages of the sag phenomena, prior to the development of significant wall-thinning at the bundle junctions; than to avoid doing so from fear of inducing channel failure.

FUTURE WORK

Future tests will assess the importance of the following factors:

- Influence of top channels: Failed channels above will add load and heat to the channel underneath, which undergoes sagging and disassembly, while the intact channels below will support some load and remove heat.
- Effect of oxidation: Dissolved oxygen in the channel material will strengthen the channel (slower creep rate), while the presence of a growing oxide layer on the outside, which is expected to crack during deformation, will decrease the load-bearing cross-section area of the tube

To address these factors, multi-channel experiments with vertically stacked channels will be performed in an inert atmosphere to understand the mechanisms involved in multiple and sequential channel deformations and failure. Also, single channel tests with various degrees of dissolved oxygen content will be used to verify or extend the applicability of creep equations developed for the inert atmosphere to model the channel behaviour in an oxidizing environment. Finally, tests in an oxidizing environment will be conducted with multiple channels so that the mechanism of channel disassembly in an oxidizing environment is understood and can be determined.

ACKNOWLEDGEMENTS

The authors wish to thank Mr. P.A. Krueger for conducting the experiments, Dr. S. Baset for pre-test modelling and Dr. R.S.W. Shewfelt for reviewing the manuscript and useful comments.

REFERENCES

1. Snell, V.G., Bonechi, M. and Kupferschmidt, W.C.H.,"Advances in Nuclear Safety", Proceedings of Pacific Basin Nuclear Conference, Seoul, Korea, Oct.29-Nov.2, 2000
2. Meneley, D.A., Blahnik, C., Rogers, J.T., Snell, V.G. and Nijhawan, S., "Coolability of Severely Degraded CANDU Cores", International Seminar on Mass and Heat Transfer in Severe Reactor Accidents, Cesme, Turkey, May 22-26, 1995
3. Rogers, J.T. and Lamari, M.L., "Transient Melting and Re-Solidification of CANDU Core Debris in Severe Accidents", Proceedings of 20th Canadian Nuclear Society Simulation Symposium, Niagara-on-the-Lake, Ontario, Canada, Sept. 7-9, 1997
4. Muzumdar, A.P., Mathew, P.M., Rogers, J.T. and Lamari, M.L., "Core Melt Retention Capability of CANDU Reactors", Proceedings of Pacific Basin Nuclear Conference, Banff, Canada, May 3-7, 1998
5. Blahnik, C., Kim, C.S., Nijhawan, S., and Thurasingham, R., "Modular Accident Analysis Program for CANDU Reactors", Proceedings of 12th Annual Conference, Canadian Nuclear Society, Saskatoon, Saskatchewan, Canada, June 9-12, 1991
6. Bonechi, M., Aziz, T., Jaitly, R., Mathew, P.M. and Stretch, A., "Generic CANDU PSA Program at AECL," IAEA Workshop on PSA Studies of PHWRs, Toronto, Canada, May 3-6, 1999
7. Shewfelt, R.S.W. and Lyall, L.W., "A High-Temperature Longitudinal Strain Rate Equation for Zr-2.5 wt% Nb Pressure Tubes", Journal of Nuclear Materials, Vol. 132 (1985)